

Towards Safe Human-Robot Interaction: Joint Impedance Control of a New Teleoperated Robot Arm

Dzmitry Tsetserukou¹, Riichiro Tadakuma², Hiroyuki Kajimoto³, Naoki Kawakami⁴, and Susumu Tachi⁵,
Member, IEEE

^{1,2,4,5} Dzmitry Tsetserukou, Riichiro Tadakuma, Naoki Kawakami, and Susumu Tachi, Department of Information Physics and Computing, University of Tokyo, Tokyo, Japan,

e-mail: dima_teterukov@ipc.i.u-tokyo.ac.jp, (tadakuma, kawakami, tachi)@star.t.u-tokyo.ac.jp

³ Hiroyuki Kajimoto, Department of Human Communications, University of Electro-Communications, Tokyo, Japan, e-mail: kajimoto@hc.uec.ac.jp

Abstract—The paper focuses on design and joint impedance control of a new teleoperated robot arm enabling torque measurement in each joint by means of incorporation of devised optical torque sensors. When the contact of arm with an object occurs, joint impedance algorithm provides active compliance of corresponding robot arm joint. Thus, the whole structure of the manipulator can safely interact with unstructured environment. In the paper, we describe detailed design procedure of the 4-DOF robot arm and optical torque sensors. To extract force signal from measured data, the gravity compensation algorithm was elaborated and verified. The experimental results of joint impedance control show that proposed strategy provides safe interaction of entire structure of robot arm with human beings and ensures the collision avoidance.

I. INTRODUCTION

Since teleoperation system was successfully developed by Goertz [1], the vast spectrum of application fields, including rescue operations, surgery, and space exploration, has been found. Typically, a slave robot controlled by the operator mainly performs the manipulations in unknown and unstructured environment. Moreover, teleoperated robot interacts with human in various cooperative tasks. In these applications, the force sensing ability is a crucial aspect of safe interaction in the environment. Recently, researchers have made a big progress in the improvement of arm contact detection ability. The NASA/DAPRA Robonaut teleoperated robot has a new tactile glove instrumented with 19 force sensors to grasp control realization [2]. In the developed system, the operator moves the robot arm until the palm contacts the object. However, the insensitive part of the robot arm still carries dangerousness for the surrounding objects. The whole-sensitive arm manipulator covered with a sensitive skin capable of detecting nearby objects was designed by V. J. Lumelsky et al. [3] to avoid collisions in time-varying environment. The sensitive skin is able to identify the point of collision rather than the external force value. As this device integrates a huge amount of small sensors incorporated in tiny rigid platform, and requires complicated wiring and signal processing hardware, the sensitive skin has high cost and reliability issues. Besides, there are some robot parts, such as elbow and shoulder joints, which are extremely difficult to cover with skin sensors. S. Morinaga and K. Kosuge [4] proposed collision detection system without using external sensors. The system recog-

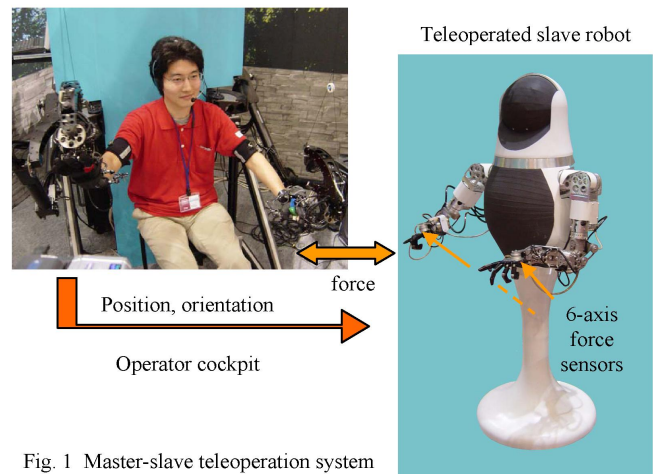


Fig. 1 Master-slave teleoperation system

nizes collisions based on the difference between the actual torque applied to the joints and the reference torque calculated from manipulator dynamics, and then generates the compliant motion in response to disturbance. However, inaccuracy and change of the dynamic model parameters deteriorate sensitivity threshold up to 17.4 N at the elbow joint. The dexterous robot-human cooperative work requires continuous precise measurement of force in range of 0-50 N.

We have successfully developed master-slave robot systems (TELESAR I and TELESAR II) based on the telepresence concept [5], and have gradually improved performance and stability of teleoperation. The operator cockpit has two 6-DOF exoskeleton-type structure arms with hands (Fig.1). The slave robot enables to perform dexterous operations by means of two 7-DOF arms and 8-DOF hands. The external force is measured through the 6-axis torque/force sensor (BL AUTOTECH MINI 4/20) attached to the robot arm wrist.

The present teleoperated robot also provides safe working area only around the wrist. To realize safe and friendly human-robot interaction, our primary idea is devoted to the design of whole-sensitive slave arm (by using distributed torque sensors in each joint) and compliant motion realization (when contact occurs). The main issue here is the cost of commercially available force/torque sensors providing redundant information for the case of only one-axis moment measurement. Moreover, to incorporate the sensors with the unique robot design, the additional mounting plates have to be installed, making the joint structure bulky. In [6], authors

described the implementation of strain-gauge-based torque sensors aimed at facilitation of torque-controlled robot. However, strain gauges have such inherent drawbacks as fragility and complicated calibration procedure. The low-pass filter is required to get readable data from these sensors because of their high sensitivity to electrical noise. The torque measurement through the elasticity of the harmonic drive flexsplines allows keeping the same stiffness of the robot [7]. This method requires the strain gauges to be installed on the flexsplines, and suffers from nonlinear behavior of the drive output shaft. In order to facilitate realization of impedance control of each arm joint, we have developed new optical torque sensors having high reliability, good accuracy, easy mounting procedure, and low price.

The first part of the paper is addressed to the description of the development of whole-sensitive robot arm and new optical torque sensors. In the second part, we discuss the procedure of gravity force estimation, the position-based impedance control algorithm, and experimental results.

II. DESIGN OF THE NEW ANTHROPOMORPHIC ROBOT ARM

In teleoperation and service application of robots, human-robot interaction is considered as crucial factor for a robot design, and imposes strict requirements on its behavior and control. From the safety point of view, to minimize injuries in case of collision, most of the robot parts were made from aluminium alloys to obtain lightweight structure, and the robot links were made with round shape reducing impact force. The distribution of the arm joints replicates the human arm structure in order to make it easy to operate using kinesthetic sensation during teleoperation.

In order to remove mechanical subsystems without disassembling the main structure when the failures do occur, we have been using a modular approach while designing anthropomorphic robot arm. Therefore, we selected CSF-series gear head type of Harmonic Drive instead of compact and lightweight component one. The Harmonic Drive offers such advantages as accurate positioning, high torque capability, torsional stiffness, and high single stage ratios. Developed teleoperated robot arm has 4-DOF. Each joint is equipped with optical torque sensor, directly connected to the output shaft of Harmonic Drive. The sizes and appearance of the arm were chosen so that the sense of incongruity during interaction with human is avoided. We kept the arm proportions the same as in average height human: upper arm length L_1 - 0.308 m; upper arm circumference - 0.251 m (diameter 0.080 m); forearm length L_2 - 0.241 m; forearm circumference - 0.189 m (diameter 0.06 m). The 3D CAD model of the developed arm and coordinate systems based on Denavit-Hartenberg convention are represented in Fig. 2.

The motors are equipped with magnetic encoders having 512 pulses per revolution. To prevent influence of bending moment and axial force on the torque value measurement, the simple supported loaded shaft configuration was implemented using couple of bearings.

The principal specifications of the developed arm are given in Table I.

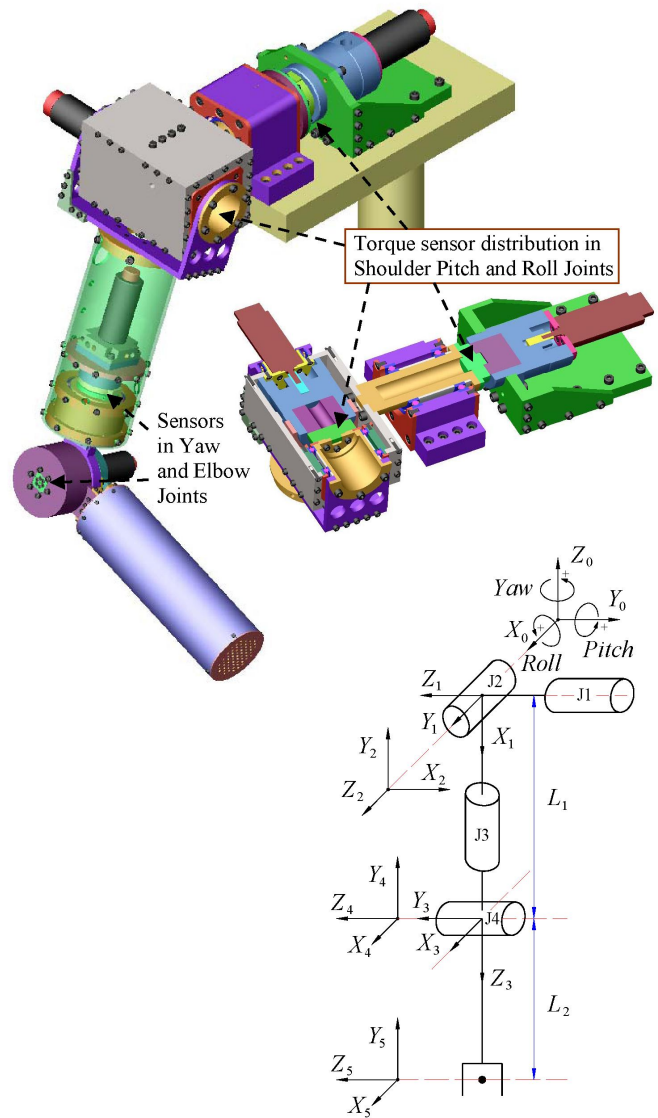


Fig. 2 3D CAD arm model and coordinate systems

TABLE I
PRINCIPAL SPECIFICATIONS

Parameters		New robot arm	
Mobility range (New robot arm/ Human arm) [deg]	Shoulder	J1, Pitch	-180 to 180 (-60 to 180)
		J2, Roll	-180 to 10 (-165 to 0)
		J3, Yaw	-180 to 180 (-60 to 180)
	Elbow	J4, Pitch	0 to 112 (0 to 130)
Motor power [W], motor type	Shoulder	J1, Pitch	90, Maxon RE 35
		J2, Roll	60, Maxon RE 35
		J3, Yaw	26.6, Faulhaber 2657
	Elbow	J4, Pitch	26.6, Faulhaber 2657
Harmonic drive rated torque [Nm], (type)	Shoulder	J1, Pitch	7.8, (CSF-14-GH)
		J2, Roll	7.8, (CSF-14-GH)
		J3, Yaw	5.0, (CSF-11-2XH)
	Elbow	J4, Pitch	5.0, (CSF-11-2XH)

III. DEVELOPMENT OF THE NEW OPTICAL TORQUE SENSOR

In our previous work, we described the techniques of the torque measurement, their advantages and shortcomings, and pointed out the motivations behind using an optical approach [8]. While designing a new optical torque sensor, we followed the guidelines listed below:

1. Addition of the torque sensor to a robot joint should cause a minimal modification in kinematics and dynamics.

2. Sensitive element should have high signal-to-noise ratio to ensure high resolution of torque measurement.
3. Mechanical structure should be machined from a single piece of metal in order to eliminate hysteresis.
4. Simple to manufacture, low in cost, and robust.

Hirose and Yoneda [9] proposed to use a split type photodiode to detect the displacement of the light source (LED). However, the output signal of this sensor is highly nonlinear. The novelty of our method is application of the ultra-small size photointerrupter (PI) RPI-121 as sensitive element [10]. We use linear section of the PI transferring characteristic to measure the shield displacement. The dimensions of the RPI-121 (3.6 mm × 2.6 mm × 3.3 mm) and its weight of 0.05 g allow realization of compact sensor design. Furthermore, PI also has small influence from the electromagnetic field and stray light. The sensor is set between the driving shaft of the harmonic transmission and driven shaft of the joint (Fig.3).

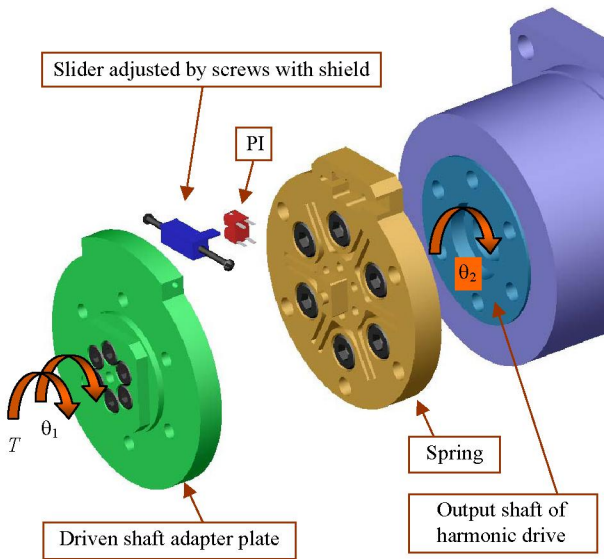


Fig. 3 Construction of the optical torque sensor

When the load is applied to the arm, the spring in corresponding joints is deflected. This causes the adapter plate rotation with small angle of twist, θ . The shield displacement is detected by the degree of interruption of infrared light that falls on the phototransistor. Thus, the magnitude of the output signal of the PI corresponds to the applied torque. The relationship between the sensed torque, T , and the angle of twist is the following:

$$T = k\theta = k(\theta_1 - \theta_2), \quad (1)$$

where k is the torsional stiffness of the spring member.

Since angle of twist is small, it can be calculated from the displacement of the shield in tangential direction, Δx :

$$T = k \Delta x / R, \quad (2)$$

where R is the distance from the sensor center to the middle axis of the shield plate in radial direction.

The sensors were manufactured from one piece of steel using wire electrical discharge machining cutting (Fig. 4).

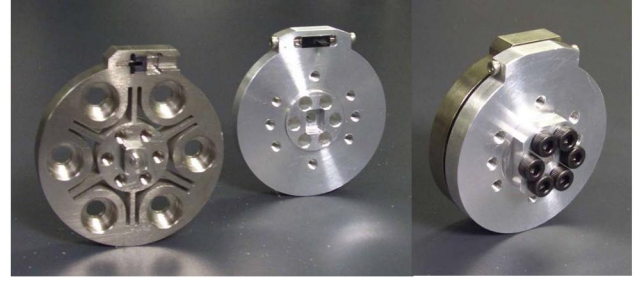


Fig. 4 Torque sensor of shoulder pitch joint

The sensor calibration results are presented in Fig. 5.

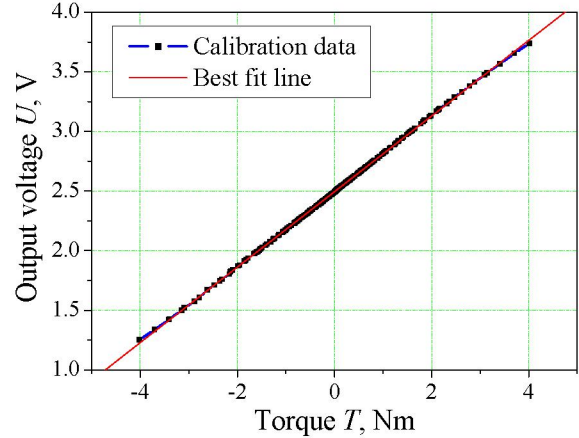


Fig. 5 Output vs. loading torque

To determine sensitivity and nonlinearity of the sensor, we used the best fit line approach. Calculated sensitivity equals to 0.317 V/Nm, and nonlinearity is 2.5 % of Full Scale. Specifications of several developed sensors and analogous 6-axis T/F sensor are listed in Table II.

TABLE II
TECHNICAL SPECIFICATION

Sensor	First joint	Second joint	Third joint Fourth joint	ATI Mini 45SI-290- 10
Sensing range, [± Nm]	12.5	10.5	4.5	10.0
Torsional stiffness, [Nm/rad]	3 230	2 730	950	35 000
Factor of safety	1.76	1.7	1.82	5.4
Outer diameter, [mm]	45.0	42.0	37.0	45.0
Thickness, [mm]	7.0	6.0	5.0	15.7
Sensor mass, [g]	70.15	50.81	34.95	92.0

The main advantages of ATI sensors [11] are high torsional stiffness and large factor of safety. Nevertheless, such features as compactness, easy manufacturing, low cost and simple calibration procedure make developed sensors preferable for torque measurement in robot arm joints.

In addition to contact force, torque sensor continuously measures the gravity load. To extract the value of the contact force from sensor signal, we elaborated the gravity compensation algorithm.

IV. GRAVITY COMPENSATION ALGORITHM AND JOINT IMPEDANCE CONTROL

A. Gravity Compensation

In this section, we consider the problem of computing the joint torques corresponding to the gravity forces acting on

links with knowledge of kinematics and mass distribution. It is assumed that due to small operation speed the angular accelerations equal zero. The Newton-Euler dynamics formulation was adopted. In order to simplify the calculation procedure, the effect of gravity loading is included by setting linear acceleration of reference frame ${}^0\dot{v}_0 = G$, where G is the gravity vector [12]. First, link linear accelerations ${}^{i+1}\dot{v}_{C_{i+1}}$ of the center of mass (COM) of each link are iteratively computed (3). Then, gravitational forces ${}^{i+1}F_{i+1}$ acting at the COM of the first and second link are computed from (4):

$${}^0\dot{v}_0 = g\hat{Z}_0; \quad {}^{i+1}\dot{v}_{C_{i+1}} = {}^{i+1}R^i \dot{v}_i \quad (3)$$

$${}^{i+1}F_{i+1} = m_{i+1} {}^{i+1}\dot{v}_{C_{i+1}}, \quad (4)$$

where m_{i+1} is the mass of the link $i+1$, ${}^{i+1}R_i$ is the matrix of rotation between successive links.

While inward iterations, we calculate force ${}^i f_i$ (5) and torques ${}^i n_i$ (6) acting in the coordinate system of each joint. In the static case, the joint torques caused by gravity forces are derived by taking Z component of the torque applied to the link (7).

$${}^i f_i = {}^{i+1}R^{i+1} f_{i+1} + {}^i F_i \quad (5)$$

$${}^i n_i = {}^{i+1}R^{i+1} n_{i+1} + {}^i P_{C_i} \times {}^i F_i + {}^i P_{i+1} \times {}^{i+1}R^{i+1} f_{i+1} \quad (6)$$

$$\tau_i = {}^i n_i^T \hat{Z}_i, \quad (7)$$

where ${}^i P_{C_i}$ is the vector locating the COM for the link i , ${}^i P_{i+1}$ is the vector locating the origin of the coordinate system $i+1$ in the coordinate system i .

The joint torques were calculated using the approach cited above. For example, for the second joint we have:

$$\tau_2 = L_{C_2} m_2 g (c_3 c_4 (c_1 c_3 s_2 + s_1 s_3) + s_3 (c_1 c_4 s_2 s_3 - c_3 c_4 s_1 - c_1 c_2 s_4)) + L_{C_1} m_1 g c_2 s_2 + L_2 m_2 g (s_3 (c_1 s_2 s_3 - c_3 s_1) + c_3 (c_1 c_3 s_2 + s_1 s_3)), \quad (8)$$

where L_{C_1} , L_{C_2} are the distances defined using 3D CAD model to the COM of the first and second link; c_1 , c_2 , c_3 , c_4 , s_1 , s_2 , s_3 , and s_4 are abbreviations for $\cos(\theta_1)$, $\cos(\theta_2)$, $\cos(\theta_3)$, $\cos(\theta_4)$, $\sin(\theta_1)$, $\sin(\theta_2)$, $\sin(\theta_3)$, and $\sin(\theta_4)$, respectively.

The plot of measured (while rotating) and calculated values of torque acting on the fourth joint is shown in Fig.6.

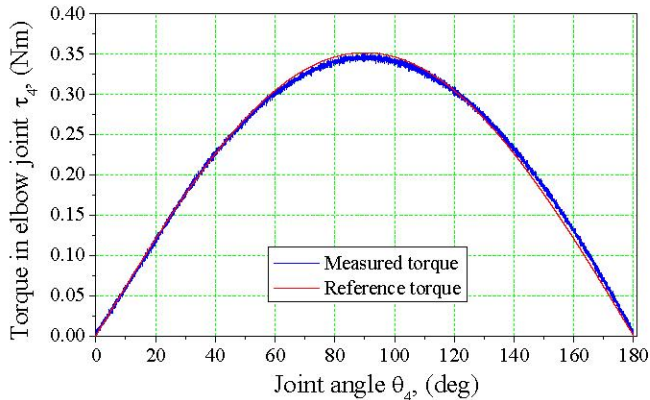


Fig. 6 Measured and referenced torques

The plot of error the torque value measurement is shown in Fig. 7. The maximum error value of 0.015 Nm is considered as threshold magnitude when contact occurs.

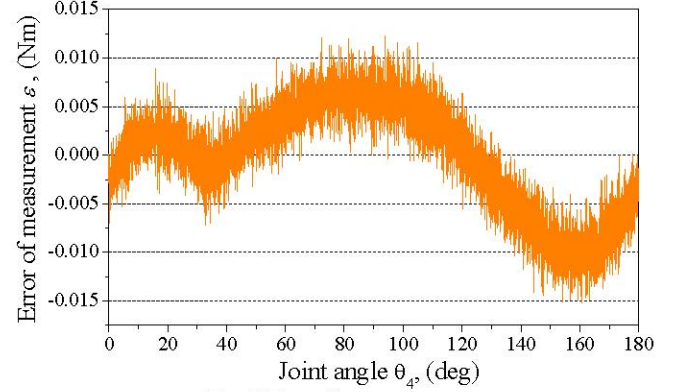


Fig. 7 Error of torque measurement

Thus, using gravity compensation algorithm we can easily determine the contact occurrence with an environment.

B. Joint Impedance Control

The dynamic equation of an n -DOF manipulator in joint space coordinates (during interaction with environment) is given by:

$$M(\theta)\ddot{\theta} + C(\theta, \dot{\theta}) + \tau_f(\dot{\theta}) + g(\theta) = \tau + \tau_{EXT}, \quad (9)$$

where θ , $\dot{\theta}$, $\ddot{\theta}$ are the joint angle, the joint angular velocity, and the joint angle acceleration, respectively; $M(\theta) \in R^{n \times n}$ is the symmetric positive definite inertia matrix; $C(\theta, \dot{\theta}) \in R^n$ is the vector of Coriolis and centrifugal torques; $\tau_f(\dot{\theta}) \in R^n$ is the vector of actuator joint friction forces; $g(\theta) \in R^n$ is the vector of gravitational torques; $\tau \in R^n$ is the vector of actuator joint torques; $\tau_{EXT} \in R^n$ is the vector of external disturbance joint torques.

People can perform dexterous contact tasks in daily activities while regulating own dynamics according to time-varying environment. To achieve such skillful behavior, the robot has to change its dynamic characteristics depending on time-varying interacting forces. The most efficient method of controlling the interaction between a manipulator and an environment is impedance control [13], [14]. This approach enables to regulate response properties of the robot to external forces through modifying the mechanical impedance parameters. The graphical representation of joint impedance control is given in Fig. 8.

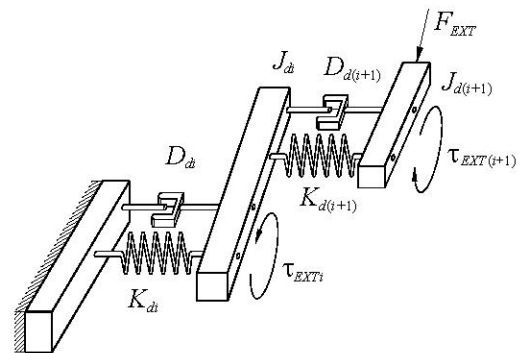


Fig. 8 Concept of the local impedance control

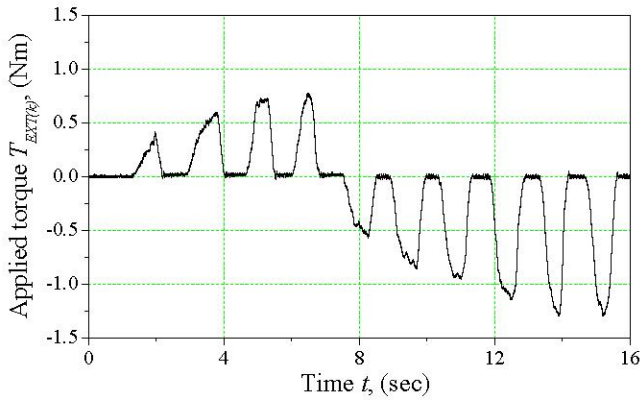


Fig. 11 Applied external torque

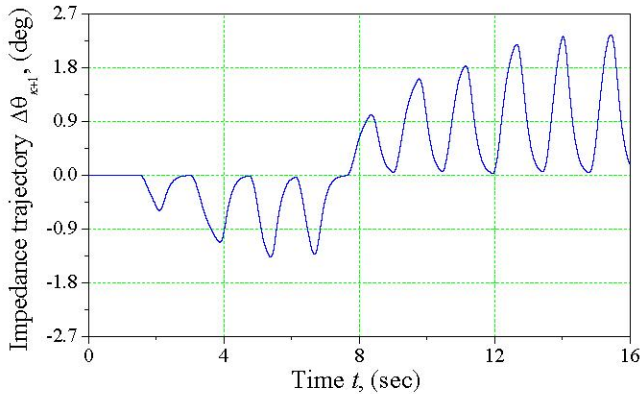


Fig. 12 Output angle of impedance model

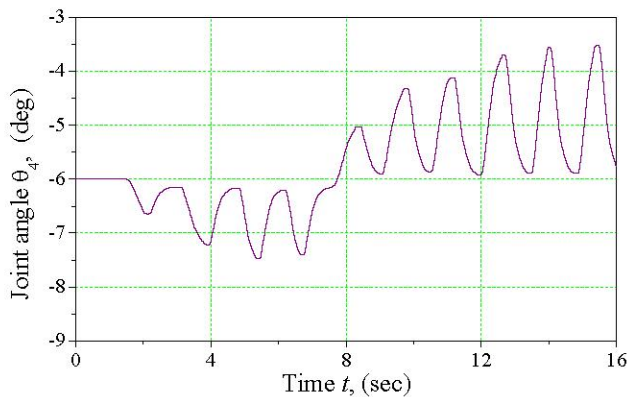


Fig. 13 Measured joint angle

The experimental results show the successful realization of joint impedance control. While contacting with human, the robot arm generates compliant motion in opposite direction to the external force vector. Thus, safety in interaction with environment is secured. As we assigned the critically damped response of impedance model to disturbance force, output angle ($\Delta\theta_{k+1}$) has ascending-descending exponential trajectory. The value of the joint impedance can easily be adjusted according to the task by selection of appropriate parameters of desired impedance model.

V. CONCLUSION AND FUTURE WORK

New whole-sensitive teleoperated robot arm was developed to provide human-like capabilities of contact task performing in a broad variety of environments. To facilitate

this arm with joint torque measuring ability, the new optical torque sensors characterized by good accuracy, high signal-to-noise ratio, and compact sizes were designed and manufactured. The effectiveness of the position-based impedance control for providing safe human-robot interaction was experimentally illustrated on a new whole-sensitive robot arm. Our next goal is realization of the intelligent variable impedance control with regard to human-robot cooperation tasks.

REFERENCES

- [1] R. C. Goertz, "Fundamentals of general purpose remote manipulators," *Nucleonics*, vol. 10, no. 11, 1952, pp. 36-42.
- [2] M.A. Diftler, C. J. Culbert, R. O. Ambrose, Jr. R. Platt, and W. J. Bluethmann, "Evolution of the NASA/DARPA Robonaut control system," in *Proc. of the 2003 IEEE Int. Conf. on Robotics and Automation*, 2003, Taipei, pp. 2543-2548.
- [3] V. J. Lumelsky and E. Cheung, "Real-time collision avoidance in teleoperated whole-sensitive robot arm manipulators," *IEEE Trans. on Systems, Man, and Cybernetics*, vol. 23, no. 1, January, 1993, pp. 194-203.
- [4] S. Morinaga and K. Kosuge, "Compliant motion control of manipulator's redundant DOF based on model-based collision detection system," in *Proc. of the 2004 IEEE Int. Conf. on Robotics and Automation*, New Orleans, LA, 2004, pp. 5212-5217.
- [5] R. Tadakuma, Y. Asahara, H. Kajimoto, N. Kawakami, and S. Tachi, "Development of anthropomorphic multi-D.O.F. master-slave arm for mutual teleexistence," *IEEE Trans. on Visualization and Computer Graphics*, vol. 11, no. 6, November, 2005, pp. 626-636.
- [6] G. Hirzinger, A. Albu-Schaffer, M. Hahnle, I. Schaefer, and N. Sporer, "On a new generation of torque controlled light-weight robots," in *Proc. of the 2004 IEEE Int. Conf. on Robotics and Automation*, Seoul, 2004, pp. 3356-3363.
- [7] M. Hashimoto, Y. Kiyosawa, and R. P. Paul, "A torque sensing technique for robots with harmonic drives," *IEEE Trans. on Robotics and Automation*, vol. 9, no. 1, February, 1993, pp. 108-116.
- [8] D. Tsetserukou, R. Tadakuma, H. Kajimoto, and S. Tachi, "Optical torque sensors for implementation of local impedance control of the arm of humanoid robot," in *Proc. of the 2006 IEEE Int. Conf. on Robotics and Automation*, Orlando, FL, 2004, pp. 1674-1679.
- [9] S. Hirose and K. Yoneda, "Development of optical six-axial force sensor and its signal calibration considering nonlinear interference," in *Proc. of the 1990 IEEE Int. Conf. on Robotics and Automation*, Cincinnati, OH, 1990, pp. 1674-1679.
- [10] Photointerrupter Design Guide, *Product catalog of ROHM*, 2005, pp. 6-7.
- [11] ATI, *Multi-axis F/T sensor*, ATI Industrial Automation, [Online], Available: <http://www.ati-ia.com>
- [12] J. Craig, *Introduction to Robotics: Mechanics and Control*, Addison-Wesley, New York: 1989, ch. 4.
- [13] N. Hogan, "Impedance control: an approach to manipulation," *ASME J. of Dynamic Systems, Measurement and Control*, 1985, pp. 1-23.
- [14] N. Hogan, "Stable execution of contact tasks using impedance control," in *Proc. of the 1987 IEEE Int. Conf. on Robotics and Automation*, Raleigh, NC, 1987, pp. 1047-1054.
- [15] R. Carelli and R. Kelly, "Adaptive impedance/force controller for robot manipulators," *IEEE Trans. Automat. Contr.*, vol. 36, no. 8, August, 1991, pp. 967-972.